ARCHIVES OF ELECTRICAL ENGINEERING VOL. 65(1), pp. 105-116 (2016)

DOI 10.1515/aee-2016-0008

Dynamic and steady state performance comparison of line-start permanent magnet synchronous motors with interior and surface rotor magnets

COSMAS OGBUKA, CAJETHAN NWOSU, MARCEL AGU

Department of Electrical Engineering
University of Nigeria, Nsukka
e-mail: cosmas.ogbuka@unn.edu.ng

(Received: 14.07.2015, revised: 28.09.2015)

Abstract: A comprehensive comparison of the dynamic and steady state performance characteristics of permanent magnet synchronous motors (PMSM) with interior and surface rotor magnets for line-start operation is presented. The dynamic model equations of the PMSM, with damper windings, are utilized for dynamic studies. Two typical loading scenarios are examined: step and ramp loading. The interior permanent magnet synchronous motor (IPMSM) showed superior asynchronous performance under no load, attaining faster synchronism compared to the surface permanent magnet synchronous motor (SPMSM). With step load of 10 Nm at 2 s the combined effect of the excitation and the reluctance torque forced the IPMSM to pull into synchronism faster than the SPMSM which lacks saliency. The ability of the motors to withstand gradual load increase, in the synchronous mode, was examined using ramp loading starting from zero at 2 s. SPMSM lost synchronism at 12 s under 11 Nm load while the IPMSM sustained synchronism until 41 seconds under 40 Nm load. This clearly suggests that the IPMSM has superior load-withstand capability. The superiority is further buttressed with the steady state torque analysis where airgap torque in IPMSM is enhanced by the reluctance torque within 90° to 180° torque angle.

Key words: PMSM, line-start, damper winding, airgap torque, reluctance torque, saliency

1. Introduction

The recent concentration of research efforts in the design, analysis and control of the Permanent Magnet Synchronous Motors (PMSM) is justified because for the same output power, PMSM offer performance enhancement over the conventional induction and synchronous motors in terms of power factor, efficiency, power density and torque-to-inertia ratio [1-7]. The performance superiority of the PMSM over the traditional induction and wound rotor synchronous motors have also been reported in [8-11]. The PMSM has also been favoured, when compared to induction motor, for line start operation, variable speed operation and in the field of semi-hermetic drives as respectively reported in [12-14].

A key issue of interest in the design of PMSM is the nature of the permanent magnet material. The properties of the permanent magnet material will affect directly the performance of the PMSM. Neodymium Iron-Boron, ($Nd_2Fe_{14}B$) is presently the best choice due its superior B-H characteristics [15]. The problem of high cost and limited supply makes supply unpredictable and researches are presently on to enhance on ferrites to achieve competitive power density and efficiency of the rare-earth PMSM [16-18].

Interior Permanent Magnet Synchronous Motor (IPMSM) and Surface Permanent Magnet Synchronous Motor (SPMSM) are the two major classes of PMSM based on the placement of the rotor permanent magnets. Surface-mounted PM motors have each of the permanent magnets mounted on the surface of the rotor, making it easy to build, and specially skewed poles are easily magnetized on this surface mounted type to minimize cogging torque. This configuration is used for low speed applications because of the limitation that the magnets will fly apart during high-speed operations. These motors are considered to have insignificant saliency, thus having practically equal inductances in both the q and d axes. The ratio between the quadrature and direct axis inductances is unity (i.e. $L_d = L_q$). Figure 1 shows the placement of rotor magnets in SPMSM [19, 20].

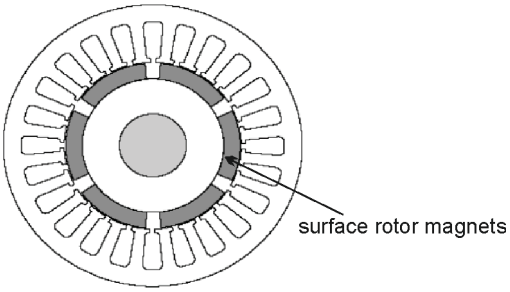

Fig. 1. SPMSM rotor assembly

IPMSM on the other hand, have rotors with interior mounted permanent magnets as shown in Figure 2.

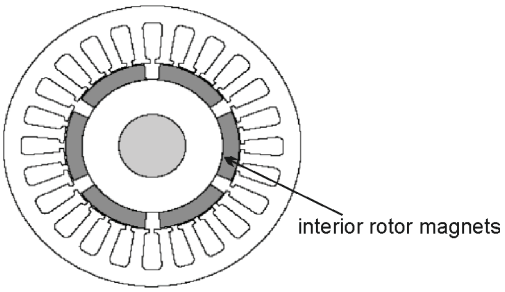

Fig. 2. IPMSM rotor assembly

Because of the internal positioning of the rotor magnets, it is good for high-speed operation. These motors have saliency with *q*-axis inductance greater than the *d*-axis inductance ($L_q > L_d$).

The magnets are very well protected against centrifugal forces [21]. Several other classifications of PMSM, based on the placement of rotor magnets, are discussed in [22]. Special rotor designs have continued to evolve to satisfy specific operational requirements.

The difference in rotor magnet placement affords the two PMSM configurations different performance characteristics. In the present study, a comprehensive dynamic and steady state comparison is made between the IPMSM and the SPMSM, of the same 4 hp rating, for line-start operation. Specifically, the run-up characteristics will be observed from rest to synchronous speed affording the opportunity to study and compare the motors within the asynchronous speed range under no load. This will be followed by two loading scenarios; (1) Step loading and (2) ramp loading to establish the load withstand capabilities of the two motors. Finally, the steady state torque characteristics of the two motors would be examined to verify the effect of the reluctance torque component associated with IPMSM as the torque angle varies. MATLAB will be used as the software tool for this research.

2. Line-Start dynamic model of PMSM

Although the industrial use of inverters for variable speed drives is widespread, constant speed line-start operation of PMSM is still dominant in medium, low, and fractional horsepower applications. The PMSM being inheritably non self starting, damper windings are employed to run the machine up to speed on induction motor action with the motor pulling into synchronism by a combination of the reluctance and synchronous motor torques provided by the magnet. During the start-up, the magnet exerts a braking torque that opposes the induction-motor-type torque provided by the damper windings. The torque provided by the damper windings must therefore overcome this magnet braking torque in addition to the load and friction, to run-up the motor successfully.

Figures 3, 4, and 5, respectively, show the q-axis equivalent circuit, d-axis equivalent circuit and the zero-sequence equivalent circuit of the Line-Start Permanent Magnet Synchronous Motor.

The following parameters are defined: v_{qs}^r = stator q-axis voltage, v_{ds}^r = stator d-axis voltage, v_0 = zero sequence voltage, i_{qs}^r = stator q-axis current, i_{ds}^r = stator d-axis current, i_0 = zero sequence current, R_s = stator resistance, ω_r = rotor speed, λ_{ds}^r = stator d-axis flux linkage, λ_{qs}^r = stator q-axis flux linkage, L_{mq} = q-axis magnetizing inductance, L_{md} = d-axis magnetizing inductance, L_{ls} = stator leakage inductance, $L_d = L_{ls} + L_{md}$, $L_q = L_{ls} + L_{mq}$, L_{lkq}^r = q-axis damper winding inductance, L_{lkd}^r = d-axis damper winding inductance, R_{kq}^r = q-axis damper winding resistance, R_{kd}^r = d-axis damper winding resistance, i_{kq}^r = q-axis damper winding current, i_{kd}^r = d-axis damper winding current, $\lambda_{af} = L_{md} i_{af}$ = magnetic flux linkage, J = moment of inertia, B = frictional coefficient.

The equivalent $qd0$ circuit of a line-start permanent magnet synchronous motor with the reference frame fixed in the rotor is shown below.

The corresponding $qd0$ dynamic equations for the motor are summarised below.

$$v_{qs}^r = R_s i_{qs}^r + p\lambda_{qs}^r + \omega_r \lambda_{ds}^r, \tag{1}$$

$$v_{ds}^r = R_s i_{ds}^r + p\lambda_{ds}^r - \omega_r \lambda_{qs}^r, \tag{2}$$

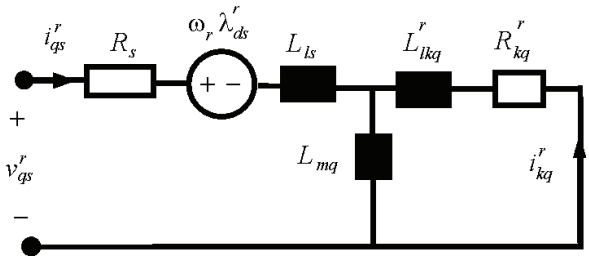

Fig. 3. *q*-axis equivalent circuit

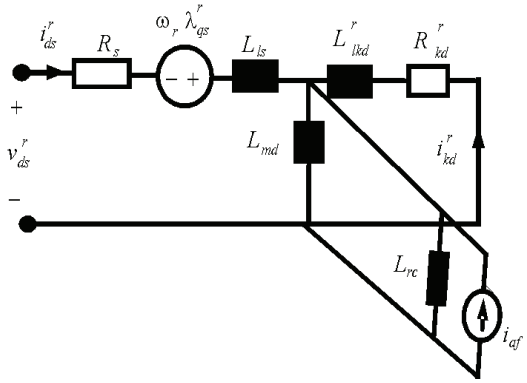

Fig. 4. *d*-axis equivalent circuit

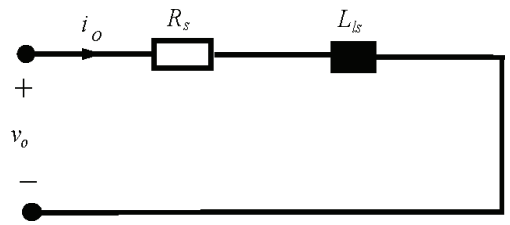

Fig. 5. Zero-sequence equivalent circuit

$$v_0 = R_s i_0 + p\lambda_0, \tag{3}$$

$$0 = R_{kd}^r i_{kd}^r + p\lambda_{kd}^r, \tag{4}$$

$$0 = R_{kq}^r i_{kq}^r + p\lambda_{kq}^r. \tag{5}$$

Flux linkages are defined as follows:

$$\lambda_{qs}^r = L_q i_{qs}^r + L_{mq} i_{kq}^r, \tag{6}$$

$$\lambda_{ds}^r = L_d i_{ds}^r + L_{md} i_{kd}^r + \lambda_{af}^r, \tag{7}$$

$$\lambda_{af}^r = L_{md} i_{af}^r, \tag{8}$$

$$\lambda_0 = L_{ls} i_0, \tag{9}$$

$$\lambda_{kq}^r = L_{mq} i_{qs}^r + L_{kq}^r i_{kq}^r, \tag{10}$$

$$\lambda_{kd}^r = L_{md} i_{ds}^r + L_{kd}^r i_{kd}^r + L_{md} i_{af}^r. \tag{11}$$

The developed electromagnetic torque is derived as

$$T_e = \frac{3}{2}\frac{P}{2}(\lambda_{af} i_{qs}^r) + \frac{3}{2}\frac{P}{2}(L_d - L_q) i_{ds}^r i_{qs}^r + \\ + \frac{3}{2}\frac{P}{2}(L_{md} i_{kd}^r i_{qs}^r - L_{mq} i_{kq}^r i_{ds}^r). \tag{12}$$

The first, second and third components of T_e are the excitation torque, reluctance torque and induction torque respectively. The damper windings are practically disengaged as soon as the rotor reaches synchronous speed. Equations 12 reduces to

$$T_e = \frac{3}{2}\frac{P}{2}[\lambda_{af} + (L_d - L_q) i_{ds}^r] i_{qs}^r. \tag{13}$$

The rotor dynamics is governed by the following set of relationships

$$T_e = J\frac{d\omega_r}{\mathrm{d}t} + T_L + B\omega_r, \tag{14}$$

$$p\omega_r = \frac{1}{J}(T_e - T_L - B\omega_r), \tag{15}$$

$$p\theta_r = \omega_r, \tag{16}$$

where P is the number of poles and $p = d/\mathrm{d}t$ is the differential operator.

2.1. Steady state torque analysis

Steady state torque characteristics of the PMSM highlights the relationship between the torque components and the torque angle δ. Assume the following set of balanced polyphase current as the input to the PMSM:

$$I_{qs} = I_m \sin(\Theta_r + \delta), \tag{17}$$

$$I_{ds} = I_m \cos(\Theta_r + \delta), \tag{18}$$

where δ is the angle between the rotor flux λ_{af} and stator current phasor and known as the torque angle since it determines the steady state torque.

Using the inverse transformation ratio $[T^r]^{-1}$,

$$[T^r]^{-1} = \begin{bmatrix} \cos\theta_r & -\sin\theta_r \\ \sin\theta_r & \cos\theta_r \end{bmatrix}. \tag{19}$$

The steady state stator current components in the rotor reference frame as shown in Figure 6 are:

$$I_{qs}^{r} = I_m \sin\delta, \tag{20}$$

$$I_{ds}^{r} = I_m \cos\delta. \tag{21}$$

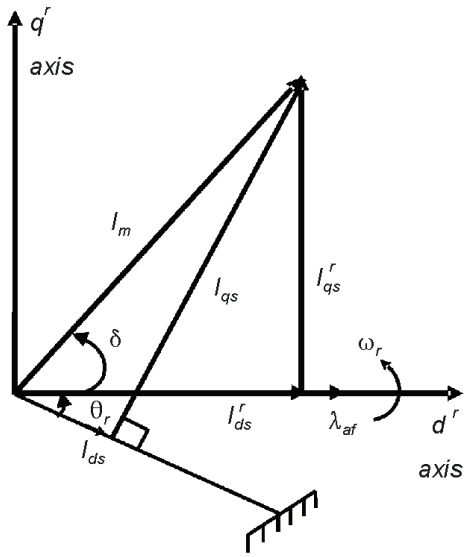

Fig. 6. Stator input current phasor diagram

Based on the Figure 6, at steady state, the airgap torque Equation (i.e. eqn. 13) becomes

$$T_e = \frac{3}{2}\frac{P}{2}[\lambda_{af} + (L_d - L_q)I_{ds}^{r}]I_{qs}^{r}. \tag{22}$$

Substituting Equations 20 and 21 into Equation 22

$$T_e = \frac{3}{2}\frac{P}{2}[\lambda_{af} I_m \sin\delta + \frac{1}{2}(L_d - L_q)I_m^2 \sin 2\delta]. \tag{23}$$

The torque angle δ directly influences the airgap torque T_e. The torque expression contains two components; the synchronous torque (excitation torque)

$$T_{es} = \frac{3}{2}\frac{P}{2}\lambda_{af} I_m \sin\delta,$$

which is due to the interaction of the rotor magnetic field and the q axis stator current and the reluctance torque

$$T_{er} = \frac{3}{2}\frac{P}{2}\frac{1}{2}(L_d - L_q)I_m \sin 2\delta,$$

due to reluctance variation.

3. Results and analysis

The parameters of the interior and surface PMSM are shown in the Appendix 1. The two motors are rated 4 Hp and operated at the rated voltage of 220 V and 50 Hz frequency. The results of the dynamic and steady state studies are presented in the plots below.

3.1. Dynamic comparison

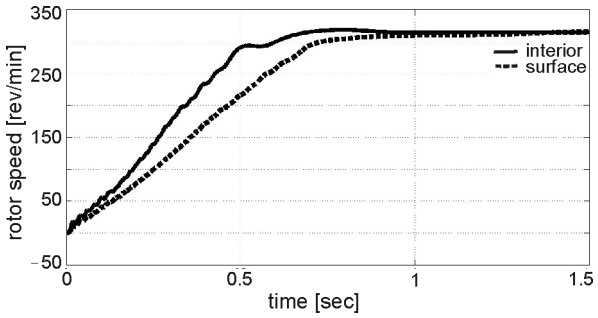

Fig. 7. Transient speed at no load

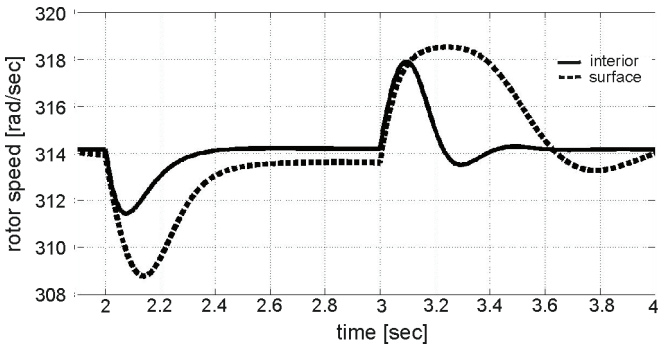

Fig. 8. Speed dynamics due to sudden load changes

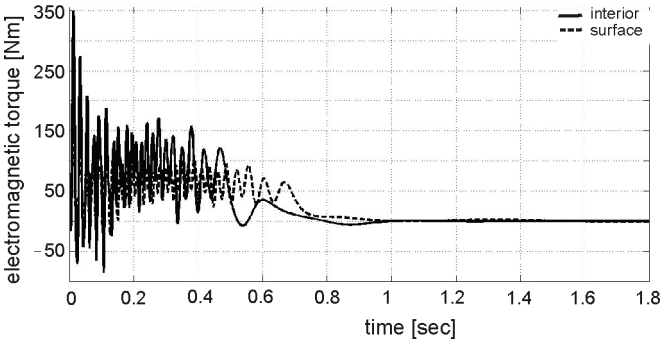

Fig. 9. Airgap torque dynamics at no load

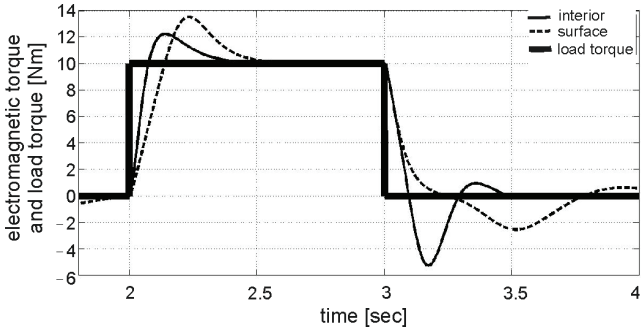

Fig. 10. Torque dynamics due to sudden load changes

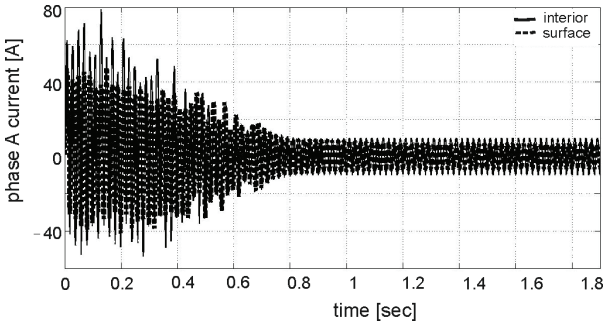

Fig. 11. Stator current transient at no load

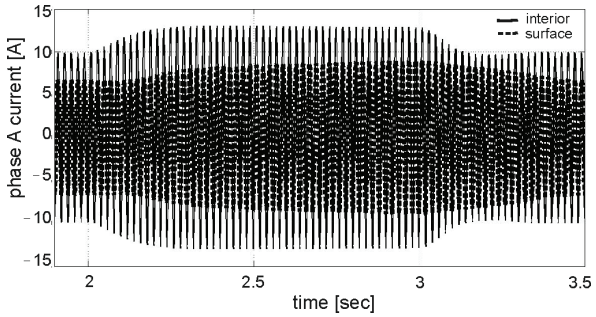

Fig. 12. Stator Current dynamics due to sudden load changes

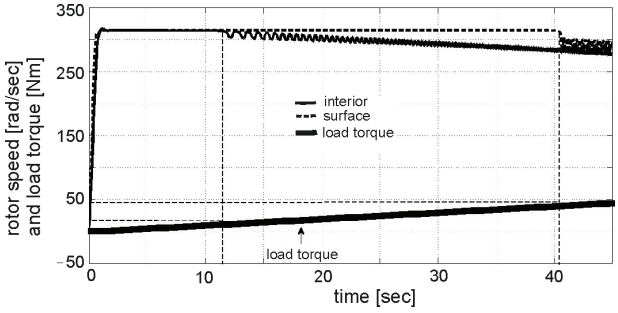

Fig. 13. Speed dynamics with ramp loading

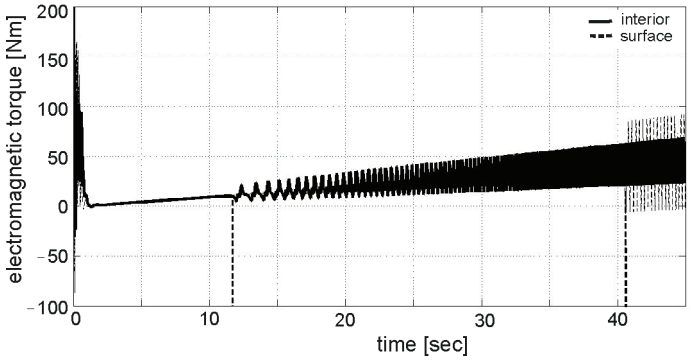

Fig. 14. Torque dynamics with ramp loading

3.2. Steady state torque comparison

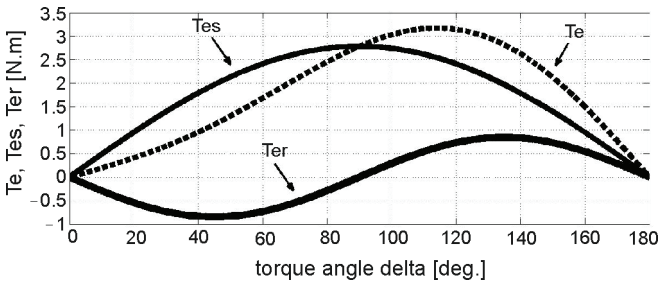

Fig. 15. Steady state torque components of IPMSM

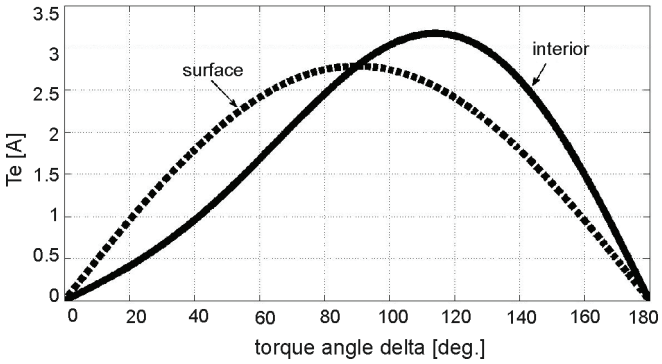

Fig. 16. Comparison of steady state torque of interior and SPMSM

The dynamic characteristics of the two motors are investigated under two scenarios. The first scenario allows the motor to run-up to synchronous speed before a step load of 10 Nm is applied at 2 s. The load is then removed suddenly at 3 s. It is seen from Figure 7 that the IPMSM synchronises faster than the SPMSM. This faster synchronisation of IPMSM is also observed during speed recovery from sudden gain or loss of load as shown in Figure 8.

From Figures 9 and 10, the airgap (electromagnetic) torque for the IPMSM is greater than that of the SPMSM below synchronous speed. This region is the asynchronous region. Upon initial attainment of synchronous speed, a combination of the excitation and the reluctance torque enables the IPMSM to quickly synchronise as shown in Figure 10. The direct proportionality between stator current and airgap (electromagnetic) torque explains the behaviour of the stator current in response to electromagnetic torque as shown in Figures 11 and 12.

The second loading scenario compares the load-withstand capabilities of the two motors as shown in Figures 13 and 14. Ramp loading is applied at 2 s (after synchronisation). Unlike the SPMSM that lost synchronism at 12 s under 11 Nm load, the IPMSM sustained synchronism until 41 s absorbing as much as 40 Nm load torque before lose of synchronism.

For the steady state torque comparison, the airgap torque and its components are plotted with a stator current magnitude of 4 A for the IPMSM as shown in Figure 15. It is noted that the peak of the airgap torque is at angle greater than 90°. The reluctance torque enhances the airgap torque only in the torque angle range from 90° to 180°; thus the preferred torque angle range of operation is between 90° to 180°. Figure 16 compares the airgap torque for the IPMSM and the SPMSM. The enhancement offered by the reluctance torque at torque range between 90° to 180° is clearly evident and this makes the peak of the torque curve to occur at angle above 90° for the IPMSM. The SPMSM has airgap torque equal to the synchronous (excitation) torque. Being a pure sinusoid, the peak of the steady state torque occurs at torque angle of 90°.

4. Conclusions

This paper has, objectively, compared the dynamic and the steady state performance of the IPMSM and the SPMSM for line-start operation under two dominant loading scenarios. Emphasis was on the run-up characteristics under no load and the response of the motors to loading upon attainment of synchronism as well as the steady state torque characteristics.

The IPMSM showed superior asynchronous performance under no load leading to a faster attainment of synchronism compared to the SPMSM. In event of sudden load change, a faster speed synchronisation is achieved in the IPMSM due to the combined effect of the excitation and the reluctance torque which forces the motor to pull into synchronism.

The ability of the motors to withstand gradual load increase was examined using ramp loading. Once again, while the SPMSM lost synchronism at 12 s under 11 Nm load, the IPMSM sustained synchronism until 41 s absorbing as much as 40 Nm load torque before lose of synchronism. The clearly suggests that the IPMSM has superior load-withstand capability compared to the SPMSM.

Finally, due to the reluctance variation in the IPMSM, the steady state torque of the IPMSM is superior to the SPMSM. Reluctance torque aids the airgap torque in the torque angle range from 90° to 180° thereby making 90° to 180° the preferred torque angle range of operation.

The outcome of this research will serve as a guide to operation engineers in taking logical decisions in the selection of machines to execute specific assignment. The design engineers

also will find the work useful in the appropriate selection of design parameters in designing PMSM to satisfy specific application area.

It is pertinent to mention that constant frequency line-start operation of PMSM is still dominant in medium, low, and fractional horsepower applications. The development of the PMSM: the design, analysis and control to provide accurate line-start capabilities will continue to occupy research attention for years to come.

Appendix: PMSM Parameters

Parameter		**IPMSM**	**SPMSM**
Rated power	Hp	4	4
Frequency	Hz	50	50
Rated phase voltage	V [Volts]	220	220
Stator resistance	R_s [Ω]	0.0906	0.2306
Magnetising flux linkage	λ_{af} [weber.turn]	0.1546	0.1546
Stator leakage inductance	L_{ls} [H]	0.0016	0.0028
d-axis magnetizing inductance	L_{md} [H]	0.0206	0.0441
q-axis magnetizing inductance	L_{mq} [H]	0.0441	0.0441
Moment of inertia	J [kgm^2]	0.4200	0.4200
No. of poles	P	6	6
Damper winding parameters			
d-axis damper leakage inductance	L^r_{lkd} [H]	0.0057	
q-axis damper leakage inductance	L^r_{lkq} [H]	0.0057	
d-axis damper resistance	R^r_{kd} [Ω]	0.7324	
q-axis damper resistance	R^r_{kq} [Ω]	1.6230	

References

[1] Cahil D.P.M., Adkins B., *The permanent magnet synchronous motor.* Proceeding of IEE (48): 483-491(1982).

[2] Weschta A., *Design considerations and performance of brushless permanent magnet servo motors.* Conference Record IAS-Annual Meeting, San Francisco, pp. 469-475 (1982).

[3] Pfaff G., Weschata A., Wick A., *Design and experimental results of a brushless ac servo drive.* Conference Record IAS-Annual Meeting, San Francisco, pp. 629-637 (1982).

[4] Demerdash N.A., Nehl T.W., *Dynamic modelling of brushless dc motors for aerospace actuation.* IEEE Transaction on Aerospace (16): 810-818(1980).

[5] Miller R.H., Nehl T.W., Demerdash N.A. et al., *An electronically controlled permanent magnet synchronous machine conditioner system for electric passenger vehicle propulsion.* Conference Record IAS-Annual Meeting, San Francisco, pp. 506-510 (1982).

[6] Maggetto G., Sneyers B., VanEck J.L., *Permanent magnet motors used for traction purposes.* Proceeding of Motorcon Conference, Oxnard California, pp. 61-68 (1982)
[7] Homer G.R., Lacey R.J., *High performance of brushless pm motors for robotics and actuator applications.* Proceeding of First European Conference. on Electrical Drives/Motor/Control, Leads, pp. 91-99 (1982).
[8] Pillay P., Krishnan R., *Modeling, simulation, and analysis of permanent-magnet motor drives I. The permanent-magnet synchronous motor drive.* IEEE Transaction Industrial Application (25): 265-27 (1989).
[9] Ong C.M., *Dynamic Simulation of Electric Machinery Using MATLAB and SIMULINK.* Prentice Hall PTR (1997).
[10] Abdel-Kader F. M., Osheba S.M., *Performance analysis of permanent magnet synchronous motors: part I: dynamic performance*, IEEE Transaction on Energy Conversion (5): 611-614 (1990).
[11] Cahill D.P., Adkin M., *The permanent magnet synchronous motor.* Proceeding of Institution of Electrical Engineering, Vol(109A): 483-491(1962).
[12] Marcic T., Stumberger B., Stumberger G. et al., *Line-starting three- and single-phase interior permanent magnet synchronous motors-direct comparison to induction motors.* IEEE Transaction on Magnetic (44): 4413-4416 (2008).
[13] Marcic T., Stumberger B., Stumberger G., *Comparison of induction motor and line-start ipm synchronous motor performance in a variable-speed drive.* IEEE Transaction on Industrial Application (48): 2341-2352 (2012).
[14] Stumberger B., Marcic T., Hadziselimovic M., *Direct comparison of induction motor and line-start IPM Synchronous Motor Characteristics for Semi-Hermetic Compressor Drives.* IEEE Transaction on Industrial Application (48): 2310-2321(2012).
[15] Krishnan R., *Permanent Magnet Synchronous and Brushless DC Motor Drives*. CRC Press Taylor and Francis Group (2009).
[16] Obata M., Morimoto S., Sanada M., Inoue Y., *Performance of pmasynrm with ferrite magnets for EV/HEV applications considering productivity.* IEEE Transaction on Industrial Application (50): 2427-2435 (2013).
[17] Sanada M., Inoue Y., Morimoto S., *Structure and characteristics of high-performance pmasynrm with ferrite magnets.* Electrical Engineering in Japan (187): 42-50 (2014).
[18] Morimoto S., Ooi S., Inoue Y., Sanada M., *Experimental evaluation of a rare-earth-free pmasynrm with ferrite magnets for automotive applications.* IEEE Transaction on Industrial Electronics (61): 5749-5756 (2014).
[19] Krishnan R., *Electric Motor Drives Modeling, Analysis, and Control.* Pearson Education (2001).
[20] Aydin M., *Axial flux mounted permanent magnet disk motors for smooth torque traction drive application.* Ph.D Thesis, Department of Electrical and Computer Engineering, University of Wisconsin (2004).
[21] Jahns T.M., *Interior permanent-magnet synchronous motors for adjustable speed drives.* IEEE Transaction on Industrial Application (22):738-746 (1986).
[22] Qinghua L., *Analysis, design and control of permanent magnet synchronous motors for wide-speed operation.* Ph.D Thesis, Department of Electrical Engineering, National University of Singapore (2005).